HHS Public Access

Author manuscript

Nat Methods. Author manuscript; available in PMC 2014 January 30.

Published in final edited form as:

Nat Methods. ; 9(4): 396–402. doi:10.1038/nmeth.1897.

Rapid optical control of nociception with an ion channel photoswitch

Alexandre Mourot[1,6], **Timm Fehrentz**[1,2,6], **Yves Le Feuvre**[3,4], **Caleb M. Smith**[1], **Christian Herold**[1], **Deniz Dalkara**[5], **Frédéric Nagy**[3,4], **Dirk Trauner**[2], and **Richard H. Kramer**[1]

[1]Department of Molecular and Cell Biology, University of California Berkeley, Berkeley, CA 94720, USA

[2]Department of Chemistry, University of Munich, Butenandtstrasse 5-13 (F4.086), D-81377 Munich, Germany

[3]CNRS, IINS, UMR 5297 'Central Mechanisms of Pain Sensitization', Bordeaux Cedex, France

[4]Université de Bordeaux, Bordeaux Cedex, France

[5]Department of Chemical Engineering, Department of Bioengineering and The Helen Wills Neuroscience Institute, University of California, Berkeley, CA, USA

Abstract

Local anesthetics are effective in suppressing pain sensation, but most of these compounds act non-selectively, inhibiting the activity of all neurons. Moreover, their actions abate slowly, preventing precise spatial and temporal control of nociception. We have developed a photoisomerizable molecule named QAQ (Quaternary ammonium – Azobenzene – Quaternary ammonium) that enables rapid and selective optical control of nociception. QAQ is membrane-impermeant and it has no effect on most cells, but it infiltrates pain-sensing neurons through endogenous ion channels that are activated by noxious stimuli, primarily TRPV1. After QAQ accumulates intracellularly, it blocks voltage-gated ion channels in the *trans* but not the *cis* form. QAQ enables reversible optical silencing of mouse nociceptive neuron firing without exogenous gene expression and can serve as a light-sensitive analgesic in rats *in vivo*. Moreover, because intracellular QAQ accumulation is a consequence of nociceptive ion channel activity, QAQ-mediated photosensitization provides a new platform for understanding signaling mechanisms in acute and chronic pain.

Correspondence and requests for materials should be addressed to RHK (rhkramer@berkeley.edu) or DT (dirk.trauner@cup.uni-muenchen.de)..

[6]Equal contribution

Author Contributions

AM and TF contributed equally to this work. AM and RHK wrote the paper. AM, TF, YLF, CMS, FN, DT and RHK designed experiments. AM, TF, YLF, CS and CH performed electrophysiological experiments and analyzed data. AM and DD performed *in vivo* experiments.

COMPETING FINANCIAL INTERESTS

The authors declare no competing financial interests.

Introduction

Optogenetic tools enable photoregulation of action potential (AP) firing in neurons, both *in vitro* and *in vivo*[1] through the introduction of exogenous genes. In contrast, small molecule photoswitches enable optical control of neuronal excitability without genetic manipulation[2,3]. Photoswitch molecules confer light-sensitivity on the intrinsic excitability of neurons within minutes[4-6]. However, unlike optogenetic tools that can be promoter-targeted for expression in particular types of neurons, photoswitches act non-selectively on all neurons that are exposed to the molecule. Depending on the scientific or biomedical application, it could be a benefit or even a requirement to target photosensitivity to a particular type of neuron.

Here we use a non-genetic strategy to target a photoswitch molecule to pain-sensing (nociceptive) neurons. Nociceptive neurons have been particularly inaccessible to selective electrophysiological manipulation, because both their peripheral sensory endings and central synaptic terminals are quite small, either embedded in the skin or interspersed with other neurons in the spinal cord. Nociceptors are unique in possessing a high density of ion channels that respond directly or indirectly to noxious stimuli[7]. For example the capsaicin receptor TRPV1, which is sensitive to noxious heat, protons and mediators of inflammation, is expressed in nociceptive neurons but it is very sparsely expressed elsewhere in the nervous system[8]. TRPV1 enters into a pore-dilated state upon prolonged agonist activation, allowing permeation of relatively large cations[9]. This property has been exploited to deliver into nociceptors a membrane-impermeant derivative of the local anesthetic lidocaine, QX-314[10].

The selective entry and silencing of nociceptors by QX-314 gives this molecule potential as a pain-selective local anesthetic[10]. However, once QX-314 enters into cells, it cannot escape and silencing persists for many hours[11]. The irreversibility of QX-314 precludes temporally precise regulation of nociceptor activity. Here we describe QAQ, a photoisomerizable molecule that confers reversible light-sensitivity selectively onto neurons involved in pain signaling, enabling rapid optical control of nociception without genetic manipulation.

RESULTS

QAQ photosensitizes voltage-gated ion channels

We have developed a photoswitch molecule, named QAQ, that suppresses excitability by optically regulating voltage-gated Na^+, Ca^{2+} and K^+ channels. QAQ has a central photoisomerizable azobenzene coupled on both sides to quaternary ammonium (QA) groups (Fig. 1a). Upon illumination with 380 nm light, the elongated *trans* QAQ converts to the bent *cis* form (Supplementary Fig. 1a). *Cis* QAQ spontaneously reverts to *trans* slowly in the dark (Supplementary Fig. 1b), but this transition occurs quickly (within ms) in 500 nm light.

QAQ resembles lidocaine and its derivative QX-314 (Fig. 1b,c), local anesthetics that block voltage-gated Na^+, K^+ and Ca^{2+} channels from the cytoplasmic side[12,13]. Lidocaine is a tertiary amine that crosses the membrane in an uncharged state and blocks ion channels after

becoming protonated in the cytoplasm. QX-314 contains a permanently charged QA, preventing it from crossing the membrane. However, QX-314 is a potent blocker of activity when introduced through a patch pipette into the cytoplasm[14].

To test whether QAQ can act like a photoregulated ion channel blocker, we made whole-cell recordings from NG108-15 cells, a mouse neuroblastoma and rat glioma hybrid cell line that expresses neuronal voltage-gated Na^+ (Na_v) channels[15]. When QAQ was delivered into the cytoplasm through the patch pipette, it blocked most of the Na^+ current in the *trans* configuration, but blockade was removed in 380 nm light (Fig. 1d). In contrast, bath application of QAQ failed to block (Supplementary Fig. 2) or photosensitize the Na^+ current (Fig. 1e), indicating that QAQ is membrane-impermeant like QX-314[10]. Light-sensitive block of the Na^+ current occurred at all membrane potentials tested (Fig. 1f). We quantified block in *trans* vs. *cis* by examining Na^+ current during a train of depolarizing stimuli. In the *trans* form, the amount of QAQ blockade is use-dependent, becoming more complete with increasing duration or frequency of depolarization (56 ± 10 % block after 30 s, $n = 7$ cells, Fig. 1g). In contrast, the *cis* form of QAQ decreased the current by 9.6 ± 0.1% ($n = 7$ cells), indistinguishable from control experiments with no QAQ (8.3 ± 0.1 %, $n = 5$ cells, $P = 0.52$ Student t-test). Photocontrol of Na^+ current could be elicited repeatedly and rapidly without decrement over many minutes (Fig. 1h and Supplementary Fig. 3).

Local anesthetics are used to silence the activity of sensory neurons, which possess a variety of voltage-gated Na^+ channels, including tetrodotoxin (TTX)-sensitive and resistant types[7]. Whole-cell recordings from rat trigeminal ganglion (TG) neurons showed that both channel types could be photoregulated by intracellular QAQ (Supplementary Fig. 4).

QAQ also photoregulates voltage-gated Ca^{2+} (Ca_v) channels. We recorded from HEK-293 cells stably expressing $Ca_v2.2$ and from GH3 cells, a rat pituitary tumor cell line expressing L-type calcium channels[16]. In both cell types, internal QAQ blocked the Ca^{2+} current in the *trans* configuration, but blockade was removed in 380 nm light (Fig. 1i and Supplementary Fig. 5a). Photoregulation of both Ca^{2+} channels was rapid, occurred at all voltages tested and exhibited little decrement over time (Supplementary Fig. 5b-f).

Voltage-gated K^+ channels are also sensitive to QAQ. We recorded from HEK-293 cells expressing the inactivation-removed Shaker K^+ channel[17] and again observed robust photoregulation, with current blocked by *trans* QAQ and unblocked by converting the molecule to *cis* (Figure 1j). QAQ block at 500 nm was steeply voltage-dependent, increasing with depolarization, as observed with other QAs[5] (Supplementary Fig. 6a). QAQ photosensitizes other voltage-gated K^+ (K_v) channels exogenously expressed in HEK-293 cells as well as native K^+ current in hippocampal neurons (Supplementary Fig. 6b-j). Photoregulation of K^+ channels occurred rapidly and without decrement over time (Supplementary Fig. 6k,l).

Hence while QAQ is normally membrane-impermeant, it photosensitizes current flowing through voltage-gated Na^+, Ca^{2+} and K^+ channels when introduced into the cell (Fig. 1k). Intracellular QAQ photosensitizes many but not all K^+ channels; K_{ir} and HCN channels are

unaffected by QAQ (Supplementary Fig. 7). Intracellular QAQ did not photoregulate current through NMDA and non-NMDA receptors (Supplementary Fig. 8).

QAQ enables photocontrol of neuronal excitability

Because it imparts light-sensitive block on voltage-gated Na^+, K^+ and Ca^{2+} channels, QAQ should have a strong influence on the electrical excitability of neurons. To examine the net effect of internal QAQ on AP firing we carried out current clamp recordings from dissociated rat hippocampal neurons in culture. Current pulses of increasing amplitude elicited a progressive increase in the number of AP when QAQ was in the *cis* configuration (Fig. 2a). However, when QAQ was converted to *trans*, neurons fired a single spike at the onset of stimulation, but failed to fire additional spikes even with the largest current pulse tested, consistent with use-dependent blockade of Na^+ channels (Fig. 2a,b). The amplitude of the first spike decreased and its half-width increased when switching from 380 to 500 nm light, in agreement with both Na^+ and K^+ channels being blocked (Fig. 2c). Higher internal concentration of QAQ (≥ 200 μM) could eliminate all spikes at 500 nm.

QAQ affects spiking but has little or no effect on the resting properties of these neurons. Neither the input resistance nor the membrane potential changed over time as QAQ diffused into the neuron (Fig. 2d,e). Moreover, light had no effect on these parameters, in agreement with QAQ not affecting K_{ir} and HCN channels, two channels that play a role in setting the resting membrane potential of neurons. Firing threshold in these neurons was the same with (195 ± 31 pA s.e.m.) and without QAQ in the pipette (161 ± 12 pA, $P = 0.44$ Student t-test) and was not affected by light (Fig. 2f).

QAQ enters cells through nociceptive ion channels

QAQ is normally membrane impermeant, so it fails to photosensitize most cells. However we asked whether QAQ could be delivered into cells without requiring dialysis through a patch electrode. This strategy involves using nociceptive pore channels as a conduit for QAQ entry. HEK-293 cells were transfected with the gene encoding the Shaker K^+ channel, which we used as an indicator of intracellular QAQ accumulation. We first used TRPV1, a channel whose pore dilates after exposure to its agonist capsaicin[9]. Control cells treated with capsaicin showed no QAQ-mediated photosensitization (Fig. 3a). However, cells expressing TRPV1 showed photosensitization of Shaker current, but only when QAQ was applied on the cells in conjunction with capsaicin. We then tested two other TRP channels, TRPA1 and TRPM8, but found no significant loading through either TRPA1 (7.3 ± 4.0 % s.e.m., $n = 11$ cells, $P = 0.39$, Student t-test) or TRPM8 channels (-0.3 ± 1.4 % s.e.m., $n = 3$ cells, $P = 0.81$, Student t-test) after these channels were activated with allyl isothiocyanate (AITC, 30 μM) or menthol (30 μM), respectively (data not shown).

Some ionotropic receptors for ATP also exhibit pore dilation upon prolonged activation[18,19]. Therefore we tested whether P2X channels could be used as a conduit for QAQ entry. Control HEK-293 cells treated with ATP showed no QAQ-mediated photosensitization (Fig. 3b). However, cells expressing $P2X_7R$ showed photosensitization of Shaker current, but only when QAQ was applied on the cells in conjunction with ATP. The amount of K^+

channel photosensitization was nearly the same 5 and 30 minutes after ATP application, suggesting that QAQ equilibrates quickly in the cell.

To test whether QAQ can enter into neurons through dilating pore channels, we recorded from cultured rat hippocampal neurons. QAQ alone had no effect on endogenous voltage-gated K^+ current (Fig. 3c). However, we could bestow light-sensitivity to neurons that exogenously expressed $P2X_7$ receptors, by treating them with QAQ and ATP. A cell death assay showed that there was no toxicity resulting from this treatment (Supplementary Fig. 9).

TRPV1 channels are crucial for nociception in peripheral sensory neurons[7,8]. The presence of endogenous TRPV1 channels suggests that QAQ might be able to enter nociceptive neurons without requiring exogenous gene expression. We examined the effect of QAQ on three different parts of nociceptive neurons; their cell bodies, located in dorsal root ganglion (DRG), their synaptic terminals, located in the spinal cord and their sensory nerve endings, located in the periphery.

Photosensitization of neurons in intact DRGs

We developed a system for recording and analyzing many mouse DRG neurons at once while simultaneously photoregulating their electrical activity (Fig. 4a**, Online Methods**). We utilized a three-dimensional multi-electrode array (MEA) containing 60 pin-shaped electrodes. We controlled the isomeric state of QAQ with a light source positioned beneath the MEA, which is transparent to 380 and 500 nm light. A suction electrode was positioned on the peripheral nerve and an external stimulation unit was used to elicit APs, which could be recorded as extracellular signals by many electrodes of the MEA (Fig. 4b). We focused on APs resulting from slowly conducting C fibers (< 2.5 $m.s^{-1}$), which specifically belong to nociceptive neurons. With the stimulating electrode 10-15 mm from the recording electrodes, spikes attributable to these neurons appear > 4 ms after the onset of the stimulus.

Following treatment with QAQ, individual electrode displayed spikes that could be silenced by switching from 380 to 500 nm light, consistent with QAQ photosensitization (Fig. 4c). This suggests that there must be some basal activity of QAQ-permeant channels in DRG neurons. The activity of 24 neurons is displayed on a raster plot (Fig. 4d). Trains of stimuli at 10 Hz elicited trains of APs, and these could also be photoregulated by switching from 380 to 500 nm light. At both wavelengths, the number of spikes diminishes within a train of stimuli, but the degree of spike train accommodation was much greater in 500 nm light.

Principal component analysis is a common method in MEA recordings for sorting spikes belonging to different neurons, depending on their stereotypical spike waveforms. However, QAQ modulates voltage-gated channels underlying APs, changing the spike waveform as a consequence of photoswitching (Fig. 4e). Therefore, instead of assigning spikes to different units, which could be particularly error-prone in this circumstance, we devised an analytical method that involves integrating the signal over a post-stimulus time window (Fig. 4e**, Online Methods**).

After treating the DRG with a high-concentration of QAQ (1 mM, 30 min), there was a dramatic decrease in the integrated signal upon switching from 380 to 500 nm light (Fig. 4f). At a lower concentration of QAQ (0.3 mM, 5 min), the integrated signal decreased by ~6 fold less upon switching wavelengths. The weak degree of photoswitching imparted on the DRG neurons by mild QAQ treatment suggests that little QAQ had accumulated in the cells.

If the TRPV1 channel is the main conduit for QAQ entry, blocking or eliminating TRPV1 channels should reduce QAQ loading, and consequently the amount of photosensitization. Consistent with this, we found that (N-(4-Tertiarybutylphenyl)-4(3-cholorphyridin-2-yl)-tetrahydro-pyrazine1(2H)-carboxamide) (BCTC), a TRPV1 antagonist that inhibits acid- and capsaicin-induced activation, significantly reduced DRG photosensitization (Fig. 4g). In $TRPV1^{-/-}$ mice, photosensitization was also strongly reduced but not completely abolished. Ruthenium red, a non-selective TRP channel pore-blocker, entirely prevented photosensitization. Taken together, these data suggest that TRPV1 channels are the main entry route for QAQ into DRGs.

This system can be used as a platform for assessing the activity of TRP channels in the intact DRG in response to various stimuli. We pre-treated the ganglia with capsaicin during QAQ loading, followed by thorough washing with normal saline. Capsaicin is a selective agonist of TRPV1, and as expected, it increases QAQ loading, and therefore photosensitization (Fig. 4g). Bradykinin (BK) is a neuropeptide that promotes pain hypersensitivity and inflammation[20]. We find that BK also promotes QAQ-mediated DRG photosensitization, consistent with a signaling cascade that leads to activation of TRP channels[21].

Surprisingly, direct electrical stimulation of sensory neuron axons in the peripheral nerve also promotes DRG photosensitization, indicating enhanced QAQ entry during the stimulation period. AP firing may directly promote QAQ entry into TRPV1-containing neurons, but TRPV1 channels are only weakly voltage-sensitive[22]. In addition, AP firing may promote DRG somata to release neuro-inflammatory transmitters, and these may indirectly lead to activation of nociceptive channels, a positive feedback mechanism that could contribute to prolonged hypersensitivity and chronic pain.

Photosensitization of neurons in spinal cord slices

TRPV1 is abundantly expressed throughout the entire length of nociceptive neurons including the central terminals in the spinal cord, but it is thought to be largely absent from non-nociceptive sensory neurons[7]. The central terminals of nociceptive neurons are located in laminae I-II of the dorsal horn of the spinal cord, whereas the terminals of non-nociceptive neurons are located in laminae III-IV[7]. If QAQ loading is selective for nociceptors, it should photosensitize only the subset of sensory neurons that terminate in laminae I-II.

We treated spinal cord slices with QAQ and recorded synaptic responses in dorsal horn neurons triggered by electrical stimulation of the dorsal root (Fig. 5a). In lamina II, the average excitatory post-synaptic current (EPSC) amplitude was significantly reduced by switching from 380 to 500 nm light (Fig. 5b) whereas light had no effect for EPSCs

recorded in lamina III-IV (Fig. 5c). These results are consistent with preferential photosensitization of nociceptive neurons by QAQ (Fig. 5d).

To distinguish between a pre- vs. post-synaptic effect of QAQ, we recorded spontaneous EPSCs in lamina II neurons and analyzed the cumulative distribution of amplitudes and inter-event interval. The amplitude of these events was unaffected by light (Fig. 5e) but the frequency was decreased by 500nm light (Fig. 5f,g) in 6 out of 8 cells. A change in EPSC amplitude indicates a post-synaptic alteration in neurotransmitter receptor function whereas a change in frequency usually indicates a change in pre-synaptic neurotransmitter release.

QAQ-mediated photosensitization also has an impact on polysynaptic pathways on the spinal cord. Trains of stimuli generated a strong inward current that persisted for several seconds after the monosynaptic EPSCs should have decayed (Fig. 5h). Switching from 380 to 500 nm light caused a dramatic reduction in the amplitude of this current. Switching back to 380 nm light largely restored the initial amplitude of the response (Fig. 5i).

In some, but not all lamina II neurons, QAQ photosensitized not only the pre-synaptic inputs but also intrinsic voltage-gated channels K^+ currents (Supplementary Fig. 10a). In contrast, there was little photosensitization of K^+ channels in laminae III-IV neurons. Photosensitization of lamina II neurons was eliminated by BCTC (Supplementary Fig. 10b). These results suggest that TRPV1 channels enabling QAQ entry are present and active in lamina II neurons to a much greater extent than in lamina III-IV neurons.

In vivo photoregulation of peripheral nerve endings

If QAQ effectively photosensitizes nociceptive neurons, light should be able to alter pain sensation *in vivo*. We explored this possibility by testing the pain-avoidance (nocifensive) blinking response that is elicited by mechanical stimulation of the cornea in rats using the von Frey hair test[23] (see details in Online Methods). The cornea is densely innervated with nociceptors[24] that mediate the blink response[23]. Free nerve endings are only a few micrometers below the surface, and the cornea is transparent, facilitating optical control. To enable QAQ entry into nociceptor nerve endings, QAQ was topically applied in conjunction with capsaicin in one eye, whereas the contralateral eye received capsaicin alone. The rats were immobilized by mild sedation with xylazine and ketamine at low doses that do not interfere with nocifensive blinking[25]. The von Frey hair test in ambient light showed that the normalized blink threshold was ~5-fold higher in the eye treated with QAQ plus capsaicin as compared to the eye treated with capsaicin alone (Fig. 6a). Moreover, 380 nm light significantly decreased the normalized blink threshold in the eye treated with QAQ plus capsaicin (Fig. 6b). The decrease in blink sensitivity caused by QAQ was completely removed by exposure to 380 nm light (Fig. 6c). Taken together, these results show that QAQ can serve as a local anesthetic that can be turned off with light.

Discussion

Microbial light-sensitive ion transporters, including halorhodopsin[26] and Arch[27], have been used as optogenetic inhibitors of neuronal activity. Genes encoding these proteins can be

promoter-targeted to subpopulations of neurons[1]. However, for several reasons, non-genetic optical control of nociception with QAQ may be preferable to optogenetic methods.

Unlike optogenetic tools that overpower the natural activity of cells, QAQ acts on endogenous ion channels that underlie initiation and propagation of APs. Hence QAQ suppresses electrical excitability at its source. Because the ion transport rate of transporters is much slower than ion flux through channels, optical silencing with halorhodopsin and Arch requires a very high expression level[1]. Exogenous expression can be achieved by injecting viral vectors into the appropriate part of the nervous system[1], but expression requires days to weeks and is restricted to neurons that are exposed to an adequate titer of virus. Optogenetic expression can result in permanent genetic alteration of neurons, which may not be necessary or desirable for the acute regulation of pain signaling, either for scientific or biomedical applications. In contrast, QAQ-mediated photosensitization occurs within minutes and persists only until the molecule dissipates, either by being metabolized inside the cell or diffusing away from targeted neurons. Because QAQ is a small molecule, it diffuses readily through tissue and presumably gains access to all neurons that have ion channels that permits its entry into the cytoplasm.

QAQ has potential value as both a scientific and a clinical tool for controlling nociception. Since it selectively accumulates in nociceptors, QAQ could selectively inhibit pain signaling while sparing other sensory modalities and therefore could function as a targeted analgesic. This is similar to the recently proposed therapeutic use of QX-314[10]. However, QAQ has the added feature of being rapidly controllable with light. *In vivo* photocontrol would require delivery of sufficient QAQ and projection of sufficient light onto target neuronal tissues. Because it is doubly charged, QAQ is unlikely to cross the blood brain barrier. But our results show that QAQ penetrates into spinal cord slices and intact DRGs, so if injected, QAQ should have access to other neural structures. Implanted fiber optic systems such as those developed for deep brain photocontrol of neurons expressing optogenetic tools[28] could be adapted for controlling QAQ administered to internal neural structures (e.g. spinal roots or DRGs). QAQ might also be controlled by an external light source following topical administration (e.g. for treating corneal pain).

QAQ-mediated photosensitization could facilitate mapping of nociceptive circuit connections mediated by fast conventional synapses or by slow neuromodulatory neurotransmitters that may contribute to central sensitization and pain hypersensitivity[20]. Our synaptic studies in spinal cord were limited to full field regulation of presynaptic activity, but higher resolution photocontrol should be possible by projecting through a microscope small spots or patterns of light, for example to target presynaptic axons or terminals.

Finally QAQ provides insight into the activity status of ion channels implicated in pain and inflammation. Previously, the activity of nociceptive ion channels was studied almost exclusively in isolated neurons that were enzymatically and mechanically dissociated from DRGs[21]. This disruptive procedure could alter the activity and levels of expression of these channels[29]. QAQ enables investigation of nociceptive ion channels activity in undisrupted neural structures. Moreover, QAQ photosensitizes regions of a nociceptor that are largely

inaccessible to electrodes. Hyperalgesia in both inflammatory and neuropathic pain is associated with up-regulation of TRP channel gene expression in peripheral nociceptors[7], however the activation status of these channels in chronic pain is unknown. Because QAQ-mediated photosensitivity is a consequence of the cumulative activity of nociceptive channels it serves as an ultra-sensitive reporter that provides new insights about when and where these channels are active, in both physiological and pathological conditions.

Online methods

General

All animals were housed in the centralized animal facilities as assigned by the University of California Berkeley and were provided food and water ad libitum. Animal care and experimental protocols were approved by the University of California Berkeley Animal Care and Use Committee. All chemicals were purchased from Sigma-Aldrich, except BCTC ((N-(4-Tertiarybutylphenyl)-4(3-cholorphyridin-2-yl)-tetrahydro-pyrazine1(2H)-carboxamide)) and AITC (Allyl isothiocyanate) that was purchased from Tocris.

QAQ synthesis and spectroscopic characterization

The synthesis of QAQ was performed as previously described[5]. UV-Vis spectra of QAQ were measured using a smartSpec Plus spectrophotometer (Bio-Rad) in combination with illumination using the Polychrome V (Till Photonics), through an optic fiber positioned perpendicular to the detection beam of the spectrophotometer.

Cell culture

HEK-293 cells were cultured under standard conditions (DMEM containing 10% FBS). We grew GH3 cells in F-12K medium containing 15% horse serum and 2.5% FBS. NG108-15 cell medium contained 95 % DMEM mixed with HAT (0.1 mM Hypoxanthine, 400 nM Aminopterin, 0.016 mM Thymidine) and 5% FBS. Cells were plated on poly-L-lysine (0.1 mg/ml) treated coverlips in a density of 12,000 cells per cm^2 for electrophysiological measurements. Dissociated hippocampal neuronal preparations were performed from neonatal Sprague Dawley rats according to standard procedures[1]. Hippocampi were dissected, dissociated and cells were plated on poly(L-lysine)-coated coverslips at a density of 100,000/cm^2. We grew hippocampal neurons in minimum essential medium containing 5% FBS, 20 mM glucose, B27 (Invitrogen), glutamine and Mito+ Serum Extender (BD Biosciences). TG neurons from neonatal rats were prepared as previously described[30]. TG were dissected, dissociated (with collagenase and trypsin) and plated on poly(L-lysine)-coated coverslips. We grew TG neurons in minimum essential medium containing 5% horse serum, MEM vitamins (Invitrogen), glutamine and Penn/Strep. HEK-293 cells were transfected using calcium phosphate precipitation and measured after 24-48 h[4]. GH3 and NG108-15 cells were recorded 24 h after plating. Hippocampal neurons were transfected at d7 and measured at d10-14. TG cells were measured 12-48 h after plating.

Dorsal root ganglia (DRG) preparation

Mice, C57/BL6 WT or $TRPV1^{-/-}$ aged 1-6 months of either sex, were deeply anaesthetized with isoflurane and killed by cervical dislocation. The spinal column and surrounding

muscle, from the sacral to cervical regions, was removed from the mouse and dissected in cold ACSF (in mM: NaCl 124, KCl 4, $MgCl_2$ 2, $CaCl_2$ 2, $NaHCO_3$ 26, glucose 20, sodium pyruvate 2, ascorbic acid 0.4,pH 7.3) equilibrated with 95% O_2-5% CO_2. A laminectomy was performed from the thorax to the sacrum, and the spinal cord was gently removed, exposing the DRG. The DRG and attached nerves (10-20 mm in length) were removed from the lumbar region, and incubated for at least 30 minutes at room temperature in an oxygenation chamber on a nitrocellulose membrane (Sartorius Stedim Biotech) moistened with ACSF.

Spinal-cord slices preparation

C57/BL6 mice were deeply anesthetized with isoflurane and quickly beheaded. The spinal column and surrounding muscles were removed and dissected in ice-cold oxygenated low calcium/low magnesium ACSF (in mM: NaCl 101; KCl 3.8; $MgCl_2$ 18.7, $MgSO_4$ 1.3; KH_2PO_4 1.2; HEPES 10; $CaCl_2$ 1; Glucose 1). After laminectomy, the spinal roots were cut, the spinal cord was gently removed and its lumbar part was placed into a small agarose block. 300 μm thick slices were prepared using a Leica VTS 1000 vibratome. The slices were then transferred in warm (31°C) ASCF equilibrated with 95% O_2 - 5% CO_2 for at least one hour before starting patch-clamp recordings.

Whole-cell electrophysiology

Patch clamp recordings of mammalian cells were performed at room temperature. Bath solution for K^+ current contained in mM: NaCl 138, KCl 1.5, $MgCl_2$ 1.2, $CaCl_2$ 2.5, tetrodotoxin 0.001 (for hippocampal neurons only), HEPES 5 and glucose 10. Bath solution for Na^+ current contained in mM: NaCl 145, $CdCl_2$ 0.5, $CaCl_2$ 2, HEPES 5 and glucose 5. Bath solution for Ca^{2+} current contained in mM: NaCl 138, KCl 5.4, $MgCl_2$ 0.8, $BaCl_2$ 20, tetrodotoxin 0.001 (for GH3 cells only), HEPES 10 and glucose 5. Bath solution for current clamp experiments contained in mM: NaCl 138, KCl 1.5, $MgCl_2$ 1.2, $CaCl_2$ 2.5, HEPES 5 and glucose 10. Pipette solution for K^+ current contained in mM: NaCl 10 mM, K^+ gluconate 135 mM, HEPES 10, $MgCl_2$ 2, MgATP 2, EGTA 1. Pipette solution for Na^+ current contained in mM: NaCl 30, CsCl 100, HEPES 10, $MgCl_2$ 2, $CaCl_2$ 1, MgATP 2, NaGTP 0.05, EGTA 10, glucose 5. Pipette solution for Ca^{2+} current contained in mM: CsCl 120, HEPES 20, $CaCl_2$ 1, MgATP 2, EGTA 11, glucose 5. Pipette solution for current clamp experiments contained in mM: NaCl 38, Kgluconate 97, HEPES 20, MgATP 4, NaGTP 0.35, EGTA 0.35. All solutions were adjusted to pH 7.4. Electrophysiological measurements were performed with an Axopatch 200A (Molecular Devices) or a Patch-Clamp PC505B (Warner) amplifier. Patch pipettes resistances varied from 2-4 MΩ. Sodium channel currents in NG108-15 cells and calcium channel currents in GH3 cells were corrected by P/N leak subtraction. pClampex 8.2 software (Molecular Devices) in combination with a Digidata 1200 interface (Molecular Devices) were used to create and apply pulse protocols. Voltage clamp recordings were low-pass filtered at 2 kHz while current clamp measurements were low-pass filtered at 5 kHz. Illumination of cells was based on a xenon lamp either in combination with narrow band-pass filters or with a monochromator Polychrome V (Till Photonics), as described[5]. For direct internal application through the patch pipette, QAQ was dissolved to a final concentration of 100 μM. Measurements were started after 5-10 min of equilibration time for HEK-293,

NG108-15, GH3 cells and TG neurons, and after 15-20 min for hippocampal neurons. For bath incubation, cells were incubated with QAQ (classically 1 mM) in the presence or absence of agonist (ATP 1-2.5 mM or capsaicin 1 μM) at 37°C in the dark. Loading solution is similar to K^+ current recording solution but with no calcium. Pretreated coverslips were rinsed with regular calcium-containing recording solution before measurement.

For spinal slice electrophysiology, slices were placed in a recoding chamber bathed with warmed (31°C) ACSF (in mM: NaCl 130.5; KCl 2.4;$CaCl_2$ 2.4; $NaHCO_3$ 19.5; $MgSO_4$ 1.3; KH_2PO_4 1.2; HEPES 1.25; glucose 10; pH 7.4) equilibrated with 95% O2 - 5% CO2.

Electrophysiological measurements were performed under the control of an Olympus BX51 microscope using an Axoclamp 2B (Molecular devices). Patch pipettes (7-11 MΩ) were filled with appropriate pipette solution (in mM: KGluconate 120; KCl 20; $CaCl_2$ 0.1; $MgCl_2$ 1.3; EGTA 1; HEPES 10; GTP 0.1; cAMP 0.2; Leupeptin 0.1; Na_2ATP 3; D-Manitol 77; pH 7.3). Illumination of preparations was performed using two different wavelength diodes (380 and 500nm) controlled by Transistor-Transistor Logic (TTL) pulses. A glass suction electrode connected to Master 8 (A.M.P.Instrument Ltd) stimulator was used to stimulate dorsal roots. Non-nociceptive primary afferent fibers were specifically recruited using low-threshold stimulations (50μs, less than 100μA) whereas nociceptive fibers were recruited using high-intensity stimulations (500μs, more than 250μA).

Multi-electrode array (MEA) Recordings

A DRG was placed onto a 3D multi-electrode array chip (MEA60 200 3D GND, Ayanda Biosystems) and secured in place with a “harp” made from dialysis membrane stretched over thick platinum wire and bonded with superglue; the wire was U-shaped to allow the nerve to exit without being crushed. The MEA chip was mounted on an MEA1060-Up amplifier (Multi Channel Systems), and placed on the stage of an IX71 inverted microscope (Olympus). The nerve was led into a manipulator-mounted glass suction electrode of appropriate size driven by a DS2 stimulus isolator (Digitimer Ltd) triggered by pClamp v10.0 software through a Digidata 1440A data acquisition system (Molecular Devices). Except during drug incubations, the MEA chamber was continuously perfused with oxygenated ACSF at ~2 ml/minute. Recordings were performed at 30°C.

Before the drug incubation, the DRG was checked for response to stimulation at 1 Hz. If the signal was acceptable, the MEA chamber solution was replaced with oxygenated ACSF containing QAQ with or without other drugs, and incubated for 5 minutes. When using blockers, the DRG was pre-incubated with the blocker for 5 minutes before the application of QAQ with the blocker. The DRG was then washed with ACSF for 10 minutes before performing the experiment.

Recordings were done at a stimulation rate of 10 Hz while illuminating the DRG with 380 nm or 500 nm light. Each experiment consisted of 5 cycles of: 30 seconds under 380 nm light followed by 30 seconds under 500 nm light. The DRG was stimulated with 1 ms pulses at 10 Hz for the last 5 seconds under each wavelength of light, allowing 25 seconds to recover from adaptation in between stimulation episodes. Illumination was provided by a U-LH100HGAPO mercury lamp (Olympus) through a 4x objective, resulting in intensities of

17-28 mW/mm^2. Filters for 380 nm and 500 nm were switched by a Lambda 10-3 system (Sutter Instrument Company) under the control of Metamorph v7.5.3.0 software (Molecular Devices). Evoked responses were recorded at 20 KHz with MC_Rack v4.0 software (Multi Channel Systems). Pictures were taken using Metamorph with a CoolSNAP HQ2 camera (Photometric) connected to the microscope.

MEA Data Analysis

Data was recorded in 40 ms-long sweeps synced to stimulation pulses, so that the stimulation produced an artifact at the beginning of the sweeps. Evoked spikes were detected by a negative threshold manually set beyond the noise level. For each detected spike, the first millisecond before the peak and the two milliseconds after were extracted into text files by MC_DataTool software (Multi Channel Systems), for processing with a custom Matlab program.

Our custom Matlab program calculated the area under each spike to the threshold level. A "region of interest" (ROI) was also set manually for each recording to exclude the stimulus artifact. The total integrated area of all spikes was calculated for each sweep, and averaged over the 5 cycles in each wavelength (Fig. 4e,f). This averaged area per sweep was summated over the 5 seconds of stimulation to quantify the total evoked response in each wavelength of light. For each active channel, the normalized photosensitization was calculated as: $(area_{380nm} - area_{500nm}) / (area_{380nm} + area_{500nm})$. Channels with excessively small and/or irregular signals were conservatively culled. The per-channel photosensitization values, generated from at least three separate DRGs per drug condition, were pooled by condition and compared for significance using a Mann-Whitney U test (5% significance level).

Cornea-evoked reflex blinks

Sprague-Dawley rats (3-6 weeks old of either sex) were sedated using intraperitoneal injection of xylazine (9 mg/kg) and ketamine (60 mg/kg). Animals were then placed on a warming pad and behavioral testing was initiated when spontaneous movements ceased, while pinching the paw with a pair of forceps elicited a brisk withdrawal reflex. We used a series of von Frey hairs, nylon fibers of increasing diameter, which are pressed against the cornea to impart increasing force of high accuracy. We held von Frey hairs perpendicular to the cornea for approximately 2 s, or until a blink is initiated, using progressive increase in force from 8 mg to a maximal value of 1 g. Stimuli were presented three times for each stiffness, at intervals of several seconds. Both eyes were tested, and a positive response was noted if the animal blinks two or three times for a given force. Capsaicin (10 μM) was then topically applied on one cornea using a pipette (10 μl volume), while the contralateral cornea was treated with a mixture of capsaicin (10 μM) and QAQ (20 mM). Von Frey testing was done again 10-15 minutes after drug application. Immediately after von Frey testing, light was applied using an LED (Prizmatix, λmax = 385 nm, 30 mW/cm^2) for one minute and von Frey hair were tested again.

Statistical analysis

Unless otherwise noted, all data are presented as ± s.e.m and statistics were analyzed with a Student t-test.

Supplementary Material

Refer to Web version on PubMed Central for supplementary material.

Acknowledgments

We thank M.R. Banghart (Harvard Medical School) and M. Kienzler (Ludwig Maximilians University Munich) for helping synthesize QAQ, S. Scott (UC Berkeley) for his help with computer programming, D. Bautista (UC Berkeley) for helpful comments, A. Nicke (Max Planck Institute of Brain Research) for the $P2X_7$ receptor clone, A. Blatz (Photoswitch Biosciences, Inc.) for HEK-293 cells stably expressing $Ca_V2.2$ and F. Ory for artistic input. This work was supported by NIH grants MH088484 to RHK and PN2 EY018241 to RHK and DT (the UC Berkeley Nanomedicine Development Center) and by the Center for Integrated Protein Science, Munich (CIPSM) to DT.

References

1. Yizhar O, Fenno LE, Davidson TJ, Mogri M, Deisseroth K. Optogenetics in Neural Systems. Neuron. 2011; 71:9–34. [PubMed: 21745635]
2. Kramer RH, Fortin D, Trauner D. New photochemical tools for controlling neuronal activity. Current Opinion in Neurobiology. 2009; 19:544–552. [PubMed: 19828309]
3. Fehrentz T, Schönberger M, Trauner D. Optochemical Genetics. Angew. Chem. Int. Ed. 2011; 50:12156–12182.
4. Fortin D, et al. Photochemical control of endogenous ion channels and cellular excitability. Nat Meth. 2008; 5:331–338.
5. Banghart MR, et al. Photochromic blockers of voltage-gated potassium channels. Angew. Chem. Int. Ed. 2009; 48:9097–9101.
6. Mourot A, et al. Tuning Photochromic Ion Channel Blockers. ACS Chem. Neurosci. 2011; 2:536–543. [PubMed: 22860175]
7. Basbaum AI, Bautista DM, Scherrer G, Julius D. Cellular and molecular mechanisms of pain. Cell. 2009; 139:267–284. [PubMed: 19837031]
8. Cavanaugh DJ, et al. Trpv1 Reporter Mice Reveal Highly Restricted Brain Distribution and Functional Expression in Arteriolar Smooth Muscle Cells. J Neurosci. 2011; 31:5067–5077. [PubMed: 21451044]
9. Chung M-K, Güler AD, Caterina MJ. TRPV1 shows dynamic ionic selectivity during agonist stimulation. Nat Neurosci. 2008; 11:555–564. [PubMed: 18391945]
10. Binshtok AM, Bean BP, Woolf CJ. Inhibition of nociceptors by TRPV1-mediated entry of impermeant sodium channel blockers. Nature. 2007; 449:607–610. [PubMed: 17914397]
11. Binshtok AM, et al. Coapplication of lidocaine and the permanently charged sodium channel blocker QX-314 produces a long-lasting nociceptive blockade in rodents. Anesthesiology. 2009; 111:127–137. [PubMed: 19512868]
12. Scholz A. Mechanisms of (local) anaesthetics on voltage-gated sodium and other ion channels. Br J Anaesth. 2002; 89:52–61. [PubMed: 12173241]
13. Hille, B. Ion Channels of Excitable Membranes. 3rd ed. Sinauer Associates Inc; 2001.
14. Strichartz GR. The inhibition of sodium currents in myelinated nerve by quaternary derivatives of lidocaine. The Journal of General Physiology. 1973; 62:37–57. [PubMed: 4541340]
15. Kawaguchi A, et al. Enhancement of sodium current in NG108-15 cells during neural differentiation is mainly due to an increase in NaV1.7 expression. Neurochem Res. 2007; 32:1469–1475. [PubMed: 17404832]
16. Rogawski MA, Inoue K, Suzuki S, Barker JL. A slow calcium-dependent chloride conductance in clonal anterior pituitary cells. J Neurophysiol. 1988; 59:1854–1870. [PubMed: 3404208]

17. Hoshi T, Zagotta WN, Aldrich RW. Biophysical and molecular mechanisms of Shaker potassium channel inactivation. Science. 1990; 250:533–538. [PubMed: 2122519]
18. Khakh BS, Bao XR, Labarca C, Lester HA. Neuronal P2X transmitter-gated cation channels change their ion selectivity in seconds. Nat Neurosci. 1999; 2:322–330. [PubMed: 10204538]
19. Virginio C, MacKenzie A, Rassendren FA, North RA, Surprenant A. Pore dilation of neuronal P2X receptor channels. Nat Neurosci. 1999; 2:315–321. [PubMed: 10204537]
20. Wang H, et al. Bradykinin produces pain hypersensitivity by potentiating spinal cord glutamatergic synaptic transmission. Journal of Neuroscience. 2005; 25:7986–7992. [PubMed: 16135755]
21. Bautista DM, et al. TRPA1 mediates the inflammatory actions of environmental irritants and proalgesic agents. Cell. 2006; 124:1269–1282. [PubMed: 16564016]
22. Voets T, et al. The principle of temperature-dependent gating in cold- and heat-sensitive TRP channels. Nature. 2004; 430:748–754. [PubMed: 15306801]
23. de Castro F, Silos-Santiago I, López de Armentia M, Barbacid M, Belmonte C. Corneal innervation and sensitivity to noxious stimuli in trkA knockout mice. Eur J Neurosci. 1998; 10:146–152. [PubMed: 9753121]
24. Rózsa AJ, Beuerman RW. Density and organization of free nerve endings in the corneal epithelium of the rabbit. Pain. 1982; 14:105–120. [PubMed: 7177676]
25. Wenk HN, Honda CN. Silver nitrate cauterization: characterization of a new model of corneal inflammation and hyperalgesia in rat. Pain. 2003; 105:393–401. [PubMed: 14527700]
26. Zhang F, et al. Multimodal fast optical interrogation of neural circuitry. Nature. 2007; 446:633–639. [PubMed: 17410168]
27. Chow BY, et al. High-performance genetically targetable optical neural silencing by light-driven proton pumps. Nature. 2010; 463:98–102. [PubMed: 20054397]
28. Zhang F, Aravanis AM, Adamantidis AR, de Lecea L, Deisseroth K. Circuit-breakers: optical technologies for probing neural signals and systems. Nat Rev Neurosci. 2007; 8:577–581. [PubMed: 17643087]
29. Malin SA, Davis BM, Molliver DC. Production of dissociated sensory neuron cultures and considerations for their use in studying neuronal function and plasticity. Nat Protoc. 2007; 2:152–160. [PubMed: 17401349]
30. McKemy DD, Neuhausser WM, Julius D. Identification of a cold receptor reveals a general role for TRP channels in thermosensation. Nature. 2002; 416:52–58. [PubMed: 11882888]

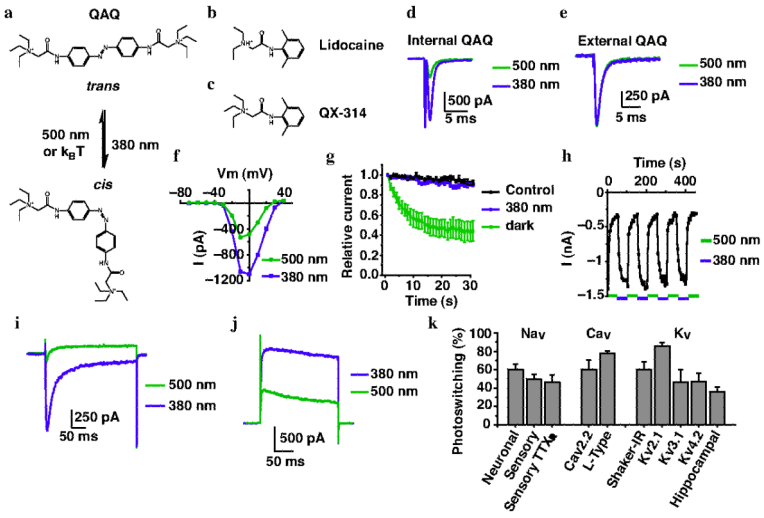

Figure 1. Intracellular QAQ photosensitizes voltage-gated ion channels

Chemical structure of (**a**) *cis* and *trans* QAQ, (**b**) lidocaine and (**c**) QX-314. k_BT = thermal energy of relaxation, with k_B = Boltzman constant and T = temperature. (**d**) Na^+ current in cells with intracellular QAQ (100 μM). Depolarization from −70 to −10 mV. Photoswitching, as defined by $(I_{380} - I_{500})/I_{380}$ = 60.5 ± 5.8 % (*n* = 4 cells) (**e**) Na current in cells with extracellular QAQ (1 mM). Photoswitching = 1.4 ± 1.3 % (*n* = 7 cells). (**f**) Current (I) *vs.* voltage (V) relationship of peak Na^+ current. (**g**) Na^+ current in cells with intracellular QAQ (100 μM) and repetitive depolarizing pulses (1Hz). Control with no QAQ is shown. (**h**) Reversibility of Na^+ current photoswitching. (**i**) $Ca_V2.2$ current using intracellular QAQ (100 μM). Depolarizing pulse from −60 to +10 mV. Photoswitching = 60.5 ± 10.5 % (*n* = 3 cells). (**j**) Shaker K^+ channel current using intracellular QAQ (100 μM). Depolarizing pulse from −70 to +40 mV. Photoswitching = 60.3 ± 8.6 % (*n* = 4 cells). (**k**) Percent photoswitching of currents through voltage-gated Na^+ (Na_V), Ca^{2+} (Ca_V) and K^+ (K_V) channels. Neuronal = Na^+ channels from NG108-15 cells; sensory = Na^+ channels from rat TG neurons; TTX_R = TTX-resistant; L-Type = Ca_V channels from GH3 cells; $Ca_V2.2$, $K_V2.1$, $K_V3.1$and $K_V4.2$ were expressed in HEK-293 cells; hippocampal = K^+ channels from primary hippocampal cultures. For all panels *n* = 3-13 cells, error bars ± s.e.m. Panels d-h refer to NG108-15 cells, panels i-j to HEK-293 cells.

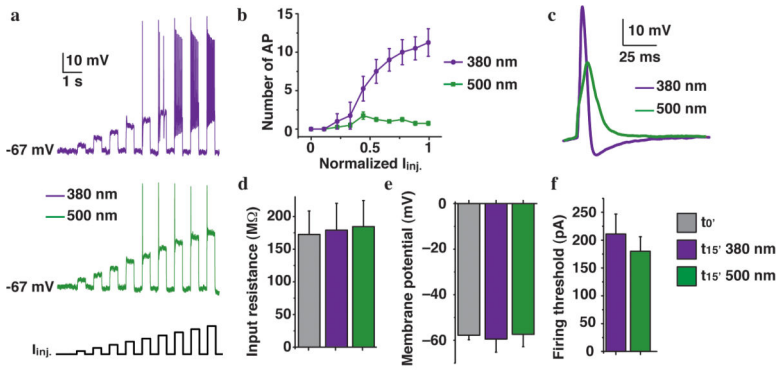

Figure 2. Intracellular QAQ is a photoswitchable inhibitor of neuronal activity

(**a**) AP firing in dissociated rat hippocampal neurons with 100 μM QAQ in the patch pipette under illumination with 380 or 500 nm light. Firing was elicited with current injections ($I_{inj.}$) of increasing amplitude. (**b**) Number of AP elicited by incremental current injections in both wavelengths. (**c**) AP shape in 380 and 500 nm light. (**d**) Input resistance at t = 0 (P = 0.86) and at t~15 min in 380 and 500 nm light (P = 0.93). (**e**) Resting membrane potential at t = 0 (P = 0.47) and at t~15 min in 380 and 500 nm light (P = 0.47). (**f**) Firing threshold in 380 and 500 nm light (P = 0.5). For all panels n = 4-6 cells; error bars ± s.e.m.; Student t-test.

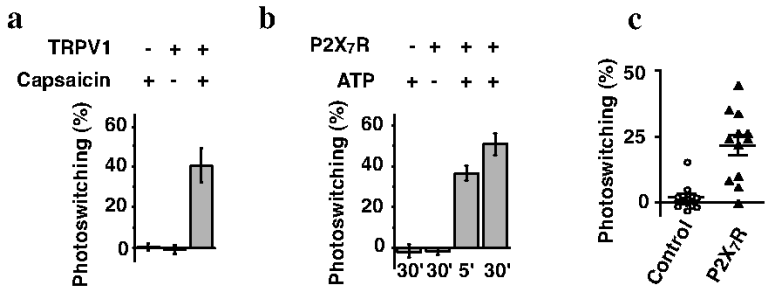

Figure 3. TRPV1 channels and P2×7 receptors serve as a conduit for QAQ entry into cells

(**a**) Percent photoswitching of Shaker K^+ channels in cells expressing (or not) TRPV1 channels and treated with or without capsaicin (1 μM) in conjunction with QAQ (30 min, 1 mM). *n* = 10 cells for each condition. (**b**) Same experiment as in a) using $P2X_7$ receptors instead of TRPV1 channels. ATP (1 mM) was applied for 5 or 30 min to activate the $P2X_7$ receptors during QAQ loading. *n* = 3-5 cells for each condition. (**c**) Percent photoswitching of native K^+ channels in hippocampal neurons. Control neurons or neurons expressing $P2X_7$ were treated for 30 min with QAQ (100 μM) plus ATP (2.5 mM). *n* = 12 cells for each condition. Error bars ± s.e.m.

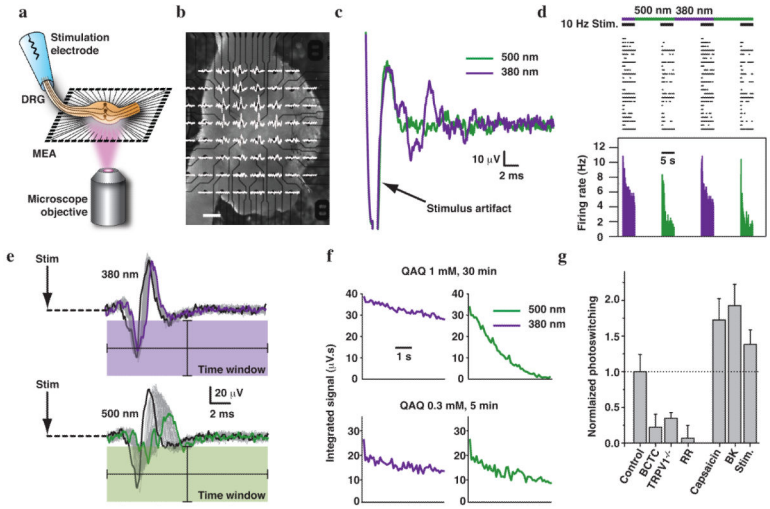

Figure 4. Photosensitization of intact DRGs recorded with a 3D MEA

(**a**) Experimental set-up. (**b**) Mouse DRG placed onto the MEA. Extracellular recordings are shown superimposed on each electrode (scale bar 200 µm). (**c**) Signals recorded from one electrode (under 380 and 500 nm light illumination) after pretreatment 30 min with 1 mM QAQ. (**d**) Simultaneous recording of 24 units. Top, raster plot of spiking under 10Hz stimulation; bottom, average firing rate (100 ms time bins). (**e**) Signals from a single electrode during a train of 50 stimuli (10 Hz). The first response is shown in black; the last in green or violet. The signal was integrated over a post-stimulus time window represented by the colored box. (**f**) Average integrated signal over five light cycles, from a DRG treated with 1 mM QAQ for 30 min or 0.3 mM QAQ for 5 min. (**g**) Quantification of photosensitization with different pretreatment conditions, normalized to photosensitization with QAQ alone (0.3 mM, 5 min). BCTC (1 µM): 22 ± 18 %, $P = 0.03$. TRPV1$^{-/-}$ mice: 34 ± 8 % photosensitization, $P = 0.005$. Ruthenium red (RR, 10 µM): 7 ± 18 % photosensitization, $P = 0.006$. Capsaicin (1 µM): 172 ± 30 % photosensitization, $P = 0.05$. BK (1 µM): 192 ± 30 % photosensitization, $P = 0.02$. Electrical stimulation (Stim; 5s-long trains of 1 ms stimuli at 10 Hz, repeated every 30 s for 5 min): 138 ± 21 % photosensitization, $P = 0.02$. Error bars ± s.e.m.; Mann-Whitney U test.

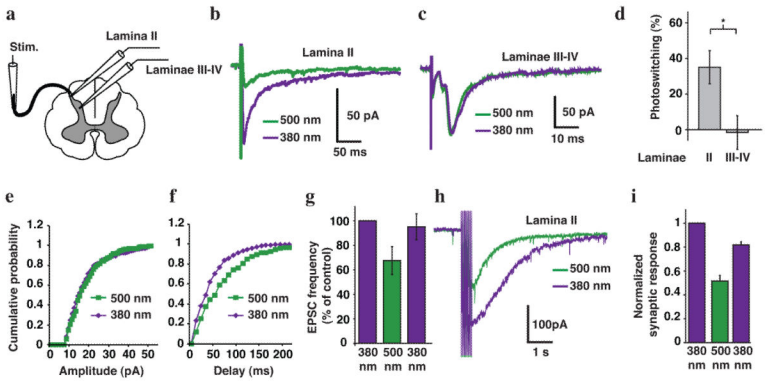

Figure 5. Photosensitization of spinal cord slices

(**a**) Schematic of a spinal cord slice with a whole-cell patch recording from neurons either in lamina II or laminae III-IV and using electrical stimulation of the dorsal root (Stim.). Postsynaptic responses recorded in a lamina II (**b**) and a laminae III-IV neuron (**c**), in response to single stimuli to the dorsal root. (**d**) Percent photoswitching of the integrated current exhibited by inputs to laminae II (35 ± 9 %, *n* = 8 cells) and III-IV neurons (-1.5 ± 9.4 %, *n* = 10 cells, $P < 0.05$). Cumulative probability distributions of EPSC (**e**) amplitude and (**f**) frequency recorded in a lamina II neuron in 380 and 500 nm light. (**g**) Average light-elicited EPSC frequency in 380, 500, and again in 380 nm light (37.5 ± 11.3 % photoswitching, *n* = 8 cells). (**h**) Polysynaptic responses recorded from a lamina II neuron in response to a 20 Hz train of stimuli to the dorsal root. (**i**) Quantification of average responses to train stimulation (50Hz, 500μs) in 11 neurons in 380, 500, and again in 380 nm light. Synaptic responses following the stimulus train were integrated and normalized to the initial amplitude in 380 nm light (*n* = 11 cells). In all panels, slices were pretreated with QAQ (1 mM for 20 min) prior to recording. Error bars ± s.e.m.; Student t-test.

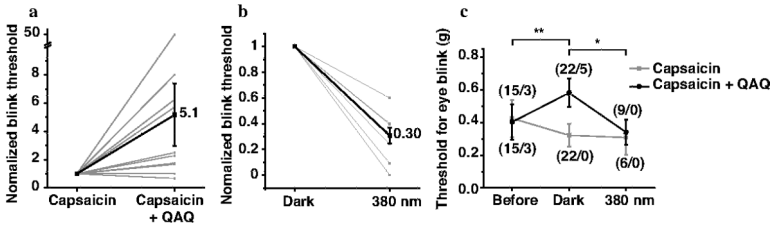

Figure 6. Light regulation of nociception *in vivo*

(**a**) Effect of QAQ on the threshold for the nocifensive blink response to mechanical stimulation of the cornea in living rats. Blink threshold in one eye treated with capsaicin alone (10 μM), and the contralateral eye treated with capsaicin plus QAQ (20 mM). Threshold, normalized to the control eye, is increased 5.1 fold (n = 22 animals, P = 0.007). (**b**) Blink threshold in the capsaicin plus QAQ eye in darkness and 380 nm light. Threshold for eye blink is decreased 3.3 fold in 380 nm compared to dark (n = 9 animals, P = 0.03). (**c**) Group data for eye blink threshold experiments. The numbers in parentheses indicate the total number of rats together with number of rats that did not respond to the maximum force applied (1 g). Error bars ± s.e.m.; Student t-test.